Ab initio Simulations of Homoepitaxial SiC Growth

M. C. Righi,* C. A. Pignedoli, R. Di Felice, and C. M. Bertoni

INFM–National Research Center on nanoStructures and bioSystems at Surfaces (S^3), Dipartimento di Fisica, Università di Modena e Reggio Emilia, Via Campi 213/A, 41100 Modena, Italy

A. Catellani

CNR-IMEM, Parco Area delle Scienze 37a, 43010 Parma, Italy

(Received 3 February 2003; revised manuscript received 30 May 2003; published 23 September 2003)

We present first-principle calculations on the initial stages of SiC homoepitaxial growth on the β-SiC(111)-($\sqrt{3} \times \sqrt{3}$) surface. We show that the nonstoichiometric reconstruction plays a relevant role in favoring the attainment of high-quality films. The motivation is twofold: On one hand, we find that the reconstruction controls the kinetics of adatom incorporation; on the other hand, we observe that the energy gain upon surface stability can induce the reorganization of the deposited material into a crystalline structure, thus revealing that a surface-driven mechanism is able to stabilize defect-free layer deposition on Si-rich surfaces.

DOI: 10.1103/PhysRevLett.91.136101 PACS numbers: 68.35.Md, 68.55.Ac, 81.15.Aa

Silicon carbide (SiC) is one of the most promising wide-band-gap semiconductors for harsh environment applications. The development of a SiC-based technology was thus far delayed because of difficulties in the materials production. We show here that some features of the growth can be successfully unraveled by *ab initio* surface calculations.

Experiments of solid-source molecular beam epitaxy (MBE) have shown that an accurate SiC layer-by-layer growth on the SiC(111) surface is possible at low temperature ($T < 1000\,^{\circ}\mathrm{C}$) under Si-stabilized conditions [1–3]. The growth mode and the film quality were found to be strongly influenced by the Si/C-flux ratio: Only by supplying excess Si, the films grew layer-by-layer and flat film-substrate interfaces were obtained. Reflection high-energy diffraction measurements performed during the experiments showed that the excess of Si supplied is employed in the formation of surface superstructures. This result suggests that the surface reconstructions may play a relevant role in determining the growth mode and the film quality.

We investigated this issue by simulating the initial stages of β-SiC growth on the SiC(111)-$\sqrt{3} \times \sqrt{3}$ surface [which contains 1/3 monolayer of excess Si adatoms with respect to an ideal Si-terminated SiC(111) crystal]: We found that the surface reconstruction influences the kinetics of adatom incorporation in such a way that a layer-by-layer growth may be favored, consistently with the suggestions of the experiments. In addition to this and as a novel result, our quasistatic quantum mechanical simulations reveal that the gain in surface energy obtained by capping the growing surface with the right dose of Si atoms to recover the $\sqrt{3} \times \sqrt{3}$ reconstruction is sufficient to activate the spontaneous transition of the system from a metastable defective configuration to the ordered crystal structure.

In order to simulate the formation of a new SiC bilayer starting from the adsorption of its elemental constituents, we performed a theoretical analysis at different levels. (i) We studied locally the *kinetics* of adatom incorporation at the SiC(111)-($\sqrt{3} \times \sqrt{3}$) reconstructed surface. To this aim, we investigated the adsorption, diffusion, and nucleation of C adatoms. The adsorption sites, corresponding to the local minima of the potential energy surface (PES) for isolated adatoms, were identified through a comparative study of the adatom binding energy at different locations. The diffusion energy barriers that the adatom has to overcome when jumping between two PES local minima were calculated by means of the nudged elastic band (NEB) method [4]. Nucleation was investigated by calculating the modifications of the adatom binding energy due to the interaction with neighboring adatoms. This kinetic analysis allowed us to predict a mechanism for the incorporation of C adatoms, and to design their possible arrangement on the surface. (ii) The successive growth phases at large dosages [one C monolayer (ML) deposition followed by the completion of the Si ML and a further 1/3 ML Si supply] were investigated globally in order to take into account long-range effects and to evaluate the surface stability in different growth conditions. To this aim, we performed a *thermodynamic* analysis of the surface free energy as a function of the chemical potential of the elemental constituents.

We performed total-energy calculations and geometry optimizations employing density functional theory within the generalized gradient approximation: We used the PW91 [5] parametrization for the exchange-correlation functional, motivated by the results of previous calculations [6]. We employed norm-conserving pseudopotentials [7] and a plane-wave basis set with a kinetic energy cutoff of 50 Ry [6]. The surfaces were modeled with periodic supercells, containing a vacuum

region 12 Å thick and a slab consisting of four SiC bilayers with a $2\sqrt{3} \times 2\sqrt{3}$ lateral unit cell (12 atoms per layer). The large in-plane size was chosen with two purposes: (i) At low coverages, it allows for the study of isolated adatoms, avoiding the interaction of an adatom with its periodic replicas; (ii) it provides a good sampling of $\sqrt{3} \times \sqrt{3}$ surfaces [8]. In this way, proper "seeds" for further nucleation may be obtained, to be used as building blocks replicated to obtain the full coverage. The slab bottom layer was passivated with hydrogen atoms. The dangling bonds of the top Si layer were saturated with four Si adatoms (Si_a) placed in the threefold sites $T4$, according to the $\sqrt{3} \times \sqrt{3}$ surface reconstruction [9,10] (a top view of our simulation supercell and a side view of the $\sqrt{3} \times \sqrt{3}$ reconstruction are shown in Figs. 1(a) and 1(b), respectively). The selected configurations were optimized by relaxing all the atomic coordinates [11] up to residual atomic forces smaller than 0.05 eV/Å.

The natural choice for simulating SiC growth at the Si-terminated surface described above is to start with the adsorption of carbon. We looked for the metastable binding locations for an isolated C adatom by locating it at the most likely adsorption sites on the surface, and then quenching the system to each nearest local minimum of the PES. The presence of the fractional Si adlayer forming the $\sqrt{3} \times \sqrt{3}$ surface reconstruction may lead to a multilevel PES for the adsorbate system, as reported for other

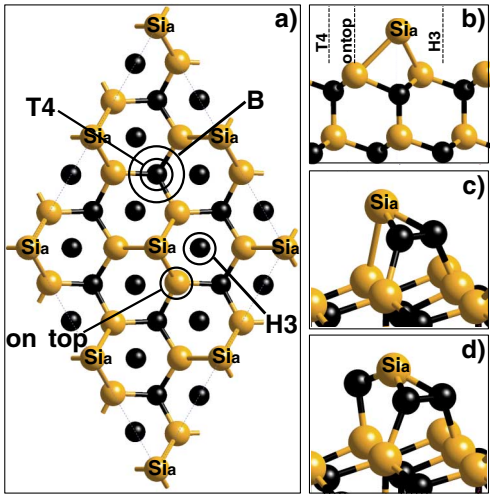

FIG. 1 (color online). (a) Top view of the $2\sqrt{3} \times 2\sqrt{3}$ cell used in the calculations and (b) side view of the $\sqrt{3} \times \sqrt{3}$ reconstruction. In (a), the in-plane position of the identified adsorption sites above the reconstruction and on the substrate surface is indicated by large and small circles, respectively. In (b), the lateral positions of B and $T4$ sites are coincident; they lie along the same vertical line, respectively above and below the Si_a adatom. Black (gray) spheres indicate C (Si) atoms, and the Si_a adatoms of the $\sqrt{3} \times \sqrt{3}$ reconstruction are explicitly labeled. Panels (c) and (d) zoom the most favorable geometries for C nucleation around one Si_a atom.

reconstructed surfaces with high corrugation [12]: Thus, we sampled locations with a different degree of the adatom incorporation into the surface. Indeed, we identified PES local minima at different depths, i.e., above and within the reconstruction.

Above the Si_a adlayer, the C adatom can adsorb in the B site [see Fig. 1(a)] at the barycenter of three Si_a atoms. Between the Si_a adlayer and the topmost substrate Si plane, instead, we identified three metastable adsorption locations: $T4$ has the same lateral position as B but is 2.0 Å lower, $H3$ and on-top are the nearest-neighbor sites of a given Si_a atom. The two latter configurations are characterized by the most favorable binding energies. In Fig. 1(a), the adsorption locations are represented on the unrelaxed surface lattice. During the structural optimization process, the C adatom almost preserves the initial lateral (x, y) positions [indicated in Fig. 1(a)], while the Si_a atoms undergo large displacements that in most cases lead to the breaking of the Si_a-Si bonds of the original surface reconstruction [13]. The fact that all four discussed sites allow for metastable configurations of isolated carbon atoms suggests that the nonstoichiometric $(\sqrt{3} \times \sqrt{3})$-SiC(111) indeed offers two adsorption channels for newly deposited C atoms: above and within the reconstruction.

We investigated the diffusion into the surface by calculating the energy barriers to be overcome by a carbon adatom when jumping from site B above the Si_a adlayer, to the other three adsorption locations below this adlayer ($H3$, $T4$, on-top). By means of the NEB method [4], we were able to find the minimum energy path (MEP) connecting the initial and final state of each diffusion process: The highest maximum along the MEP defines the energy barrier. The initial and final states correspond to the optimized adsorption geometries obtained before. The computed values indicate that the diffusion from B to on-top is activated with the low energy cost of about 0.16 eV, while the energy barriers for carbon diffusion from B to $H3$ and $T4$ are about 1 order of magnitude higher. This result reveals that at the ordinary growth temperatures the deposited C atoms have a high probability to penetrate into the $\sqrt{3} \times \sqrt{3}$ reconstruction by jumping from the B site into the on-top site. This preferred diffusion channel favors the occupation of the correct zinc blende sites above the topmost complete (111) plane of Si atoms. We also evaluated the energy barriers for adatom diffusion within the reconstruction and found that the diffusion towards $T4$ is highly improbable with respect to the diffusion processes occurring around each Si_a between the nearest-neighbor sites $H3$ and on-top: When jumping from $H3$ to on-top and vice versa, the C adatom can preserve its lateral coordination as the C-Si_a bond remains intact. This anisotropic diffusion causes the C adatoms that are present on the surface to spend most of the time around the Si_a atoms, which thus act as nucleation centers.

We therefore investigated the nucleation around each Si_a by supplying further C atoms at the on-top and $H3$ sites surrounding the Si_a atom at the center of our simulation supercell [see Fig. 1(a)]. Starting from the relaxed geometries obtained after the adsorption of one C atom at $H3$ and on-top sites, we added a second C adatom at a new on-top or $H3$ site, and we let the system relax. We took into account all the ways to occupy two of the six Si_a nearest-neighbor lattice sites that are compatible with the bond counting rule. The same procedure was followed to simulate the adsorption of three C atoms, thus completing the coverage of one of the four $\sqrt{3} \times \sqrt{3}$ patches in the simulation cell. Comparing the binding energy per C atom [14] of the different simulated C-Si_a clusters, we found that the most stable configurations are those in which only on-top sites are occupied. These structures are shown in Figs. 1(c) and 1(d): When two C adatoms are located at on-top sites, they interact attractively and a C-C double bond (1.34 Å) is established after structural relaxation. The energy gained in dimer formation with respect to the adsorption of individual C atoms in two isolated on-top sites is 1.7 eV/atom, the stability of the on-top site is thus enhanced by C-C interaction. This mechanism introduces defects in the crystal structure and hinders the attainment of ordered SiC phases. The clusterized structure of Fig. 1(d) suggests a growth scenario in which an exchange mechanism is at work: The deposited C atoms penetrate into the surface reconstruction pushing up the Si_a atom that floods on top of the surface saturating C dangling bonds.

Because of the efficiency of Si_a as a nucleation center that can accommodate up to three C atoms, and to the stability of the "3 on-top" structure [Fig. 1(d)], we simulated the full C ML in only one geometry obtained by replicating the local "3 on-top" arrangement of Fig. 1(d) to cover the whole $2\sqrt{3} \times 2\sqrt{3}$ cell. In this case, after relaxation, the surface layout, depicted in Fig. 2(a), presents C atoms bonded to Si atoms of the substrate with almost vertical bonds: This is a promising situation for the formation of a new SiC bilayer. However, this is a defective C monolayer because of the presence of C-C dimers, which change the geometry with respect to the bulk C planes.

We examined if and how the chemical bonds at this defective nonstoichiometric surface change after the completion of a full Si ML, which recovers the SiC stoichiometry. Indeed, one would hope that, in the presence of a full ML of Si atoms arranged above the C adlayer at the correct zinc blende sites ($H3$), the C-C dimers would break to favor the formation of a β-SiC bilayer. This is not the case: The deposited Si atoms do not adsorb closely to the substrate and remain about 0.9 Å above the C atoms (instead of 0.4 Å in the ideal case); the latter preserve their original arrangement with planar C-C bonds. Being attached to C dimers, the Si adatoms are dragged towards each other and form Si-Si lateral bonds,

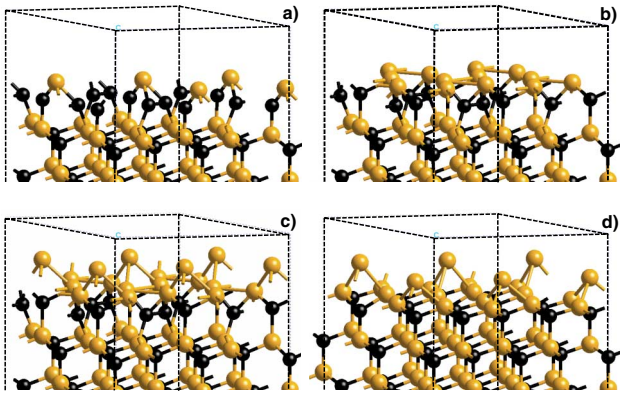

FIG. 2 (color online). Optimized surface geometry after the deposition of one C ML on the $(\sqrt{3} \times \sqrt{3})$-SiC(111) surface (a), and after the subsequent Si adlayer completion by adding 2/3 ML of Si (b). In the last two snapshots, the surface configuration obtained by further deposition of 1/3 ML of Si is represented before (c) and after (d) the relaxation process. The C-C and Si-Si planar bonds are still present in (c) and are destroyed in (d) to recover the $\sqrt{3} \times \sqrt{3}$ Si-rich reconstruction.

as seen in Fig. 2(b). We conclude that C-C bonds are very stable and the deposited Si atoms are not reactive enough to enable C-C dissociation. The C dimers remain buried under the Si adlayer, inducing the attainment of a stoichiometric SiC film far away from the desired bulk symmetry.

The most interesting and outstanding result is found when further Si atoms are added in the amount of 1/3 ML, uniformly distributed at $T4$-like sites on the disordered stoichiometric surface [see Fig. 2(c)]. During the structural optimization process, an impressive cooperative rearrangement of all the atoms belonging to the three outermost layers occurs: The C-C and Si-Si bonds are spontaneously broken to form the C-Si bonds of a perfect SiC bilayer. Furthermore, the Si topmost adatoms chemisorb above such a bilayer according to the Si_a-adatom $\sqrt{3} \times \sqrt{3}$ reconstruction geometry forming a fractional ML equivalent to the original layer of Si_a atoms [the optimized structure is shown in Fig. 2(d)]. We may explain the above result by assuming the existence of an energy barrier, probably associated with C-C and Si-Si bond dissociation, which hinders the spontaneous transition of the system from the disordered stoichiometric surface of Fig. 2(b) to the ideal SiC(111), which is indeed a nonconventional SiC surface termination. The free energy gained when the surface is stabilized by the fractional Si adlayer forming the $\sqrt{3} \times \sqrt{3}$ reconstruction is sufficient to activate the transition, and the system is not trapped in a disordered local minimum. Charge redistribution towards the formation of Si-C polar bonds, and saturation of the surface dangling bonds via the adatom reconstruction, stabilizes the new structure and the ordered stacking of Si-C bilayers.

The identified reconstruction-driven mechanism can work if the energy gain is enough to activate the transition

from the defective to the crystalline phase. This of course depends on the effectiveness of the particular reconstruction in stabilizing the surface, and on the stability of the intervening disordered phases. To better understand this point, we compared the surface energies of the configurations explored during our simulation of alternate C and Si deposition. In equilibrium conditions with bulk SiC, the surface energy is a function of the chemical potential of the C species only, which varies in a physical range determined by the values of the chemical potentials of bulk Si and bulk C [15]. The $\sqrt{3} \times \sqrt{3}$ reconstructed surface, which is our initial and final condition, has a much lower energy than the 1×1 surface (-1.2 and -1.8 eV per $\sqrt{3} \times \sqrt{3}$ in C- and Si-rich conditions, respectively), in agreement with previous computational results [6,9]. After the deposition of one C ML, the surface becomes extremely unstable and, even when the SiC stoichiometry is realized, by means of additional Si deposition, the surface energy is still high and the system is trapped in a disordered stoichiometric phase predicted to be less stable than the ideal 1×1 ($+3.5$ eV/$\sqrt{3} \times \sqrt{3}$ unit cell): The presence of C-C and Si-Si bonds in the structure induces a considerable stress at the surface. Thus, in the present case the defective dimerized configuration is a shallow minimum and the surface stabilization via the $\sqrt{3} \times \sqrt{3}$ reconstruction induces a huge energy gain.

We expect that the results obtained on the growth of 3C-SiC can be generalized to the hexagonal polytypes because the $\sqrt{3} \times \sqrt{3}$ is a stable phase not only for 3C but also for the 4H and 6H SiC(0001) surfaces. It has been shown that the cubic stacking is favorable in the vicinity of the $\sqrt{3} \times \sqrt{3}$ reconstructed SiC surface, independently of the underlying polytype, and that hexagonal-to-cubic transition may be induced through ordered deposition [6,10]. Therefore, we suggest that the zinc blende polytype analyzed in this work is well representative of the surface phenomena, because (i) it is the most favorable surface stacking and (ii) the surface energy differences between different polytypes are small with respect to the energy gain upon disorder-to-order transition.

In conclusion, we simulated the formation of a new SiC crystalline bilayer on SiC by means of alternate C and Si deposition on the $\sqrt{3} \times \sqrt{3}$ SiC(111) surface. We have shown that the presence of the Si-rich surface reconstruction favors the attainment of high-quality SiC films, as observed experimentally. We have identified two relevant effects. First, the reconstruction controls the kinetics of adatom incorporation into the SiC(111) surface: The local environment of the $\sqrt{3} \times \sqrt{3}$ reconstruction shapes a multilevel PES that favors the channeling of impacting C atoms towards the correct crystalline sites. Moreover, the anisotropic subsurface C diffusion, along with the observed C-C interactions, favors the nucleation around each Si_a adatom. The formation of a high density of nuclei may favor layer-by-layer growth, as observed, e.g., for metallic surfaces. Second, the strong energy gain upon surface stabilization induces the reorganization of the underlying disordered layers into the ordered crystal structure. Therefore, we suggest that growth techniques, such as atomic layer epitaxy, that allow for surface superstructures to be stabilized during growth, could favor the formation of defect-free layers in SiC homoepitaxy.

C. Cavazzoni is gratefully acknowledged for computational aid. Funding was provided by INFM through PRA-1MESS and by MIUR through FIRB-NOMADE. Computer time was available at the CINECA facilities through the INFM Parallel Computing Initiative.

*Electronic address: mcrighi@unimore.it

[1] A. Fissel, B. Schröter, and W. Richter, Appl. Phys. Lett. **66**, 3182 (1995).
[2] A. Fissel, U. Kaiser, E. Ducke, B. Schröter, and W. Richter, J. Cryst. Growth **154**, 72 (1995).
[3] A. Fissel, U. Kaiser, K. Pfennighaus, B. Schröter, and W. Richter, Appl. Phys. Lett. **68**, 1204 (1996).
[4] G. Henkelman and H. Jonsson, J. Chem. Phys. **113**, 9901 (2000).
[5] J. P. Perdew, J. A. Chevary, S. H. Vosko, K. A. Jackson, M. R. Pederson, D. J. Singh, and C. Fiolhais, Phys. Rev. B **46**, 6671 (1992).
[6] M. C. Righi, C. A. Pignedoli, G. Borghi, R. Di Felice, C. M. Bertoni, and A. Catellani, Phys. Rev. B **66**, 45320 (2002).
[7] N. Troullier and J. L. Martins, Phys. Rev. B **43**, 1993 (1991).
[8] Consistently with the use of large supercells, only the Γ point was included in the Brillouin-zone sums. The accuracy of this choice was proven to quantitatively reproduce the stability of the well-known Si-adatom $\sqrt{3} \times \sqrt{3}$ reconstruction with respect to other possible geometries.
[9] J. E. Northrup and J. Neugebauer, Phys. Rev. B **52**, R17001 (1995).
[10] U. Starke, J. Schardt, J. Bernhardt, M. Franke, and K. Heinz, Phys. Rev. Lett. **82**, 2107 (1999).
[11] C. Cavazzoni and G. L. Chiarotti, Comput. Phys. Commun. **123**, 56 (1999).
[12] A. Kley, P. Ruggerone, and M. Scheffler, Phys. Rev. Lett. **79**, 5278 (1997).
[13] The details of the optimized adsorption geometries together with the detailed description of C diffusion are beyond the scope of this report and will be thoroughly discussed in a forthcoming paper.
[14] The binding energy per atom e_b is defined by the following relation: $e_b = 1/N(E_{\text{tot}} - E_0 - Ne_a)$, where E_{tot} (E_0) is the total energy of the system after (before) the adsorption of N atoms; e_a is the energy of the isolated atom.
[15] G.-X. Qian, R. M. Martin, and D. J. Chadi, Phys. Rev. B **38**, 7649 (1988).